A Sphere Eversion Using Ruled Surfaces and Its Parameters

Benjamin Li

Abstract

In this paper I define sphere eversion and explore a specific sphere eversion that uses ruled surfaces and was discovered by Adam and Witold Bednorz. I also examine how each parameter in their paper modifies the eversion.

1 Introduction

A sphere eversion is a process by which a sphere can be continuously deformed inside out without creating any creases. Smale proved that such a process exists in [6]. However, only later were explicit examples of sphere eversion described. One such example, in which ruled surfaces were used, was described by Witold and Adam Bednorz in [1] and will be discussed in this paper in sections 3 and 4. Finally, [5] is a helpful website for visualizing the process described by [1]. All figures were made using Mathematica.

2 Definition of Sphere Eversion

Assuming basic knowledge of differential geometry, we start with the definition of a homeomorphism.

Definition 2.1. *Suppose there is a $X \subseteq \mathbb{R}^m$ and a $Y \subseteq \mathbb{R}^n$. A function $f : X \to Y$ is a homeomorphism if f is a bijection and if both f and f^{-1} are continuous.*

We now introduce the formal definition of a manifold given by [4].

Definition 2.2. *An n-manifold M is a Hausdorff space with a countable basis such that for all $\mathbf{p} \in M$, there exists a neighborhood of $\mathbf{p}$ that is homeomorphic to an open subset of $\mathbb{R}^n$.*

In the context of sphere eversion and this paper, however, we are only interested in 2-manifolds, which are surfaces. Here, surfaces can be thought of as subsets of $\mathbb{R}^3$ that are locally homeomorphic to $\mathbb{R}^2$. We can now define an immersion, from [2].

Definition 2.3. *A smooth map $f : M \to N$, where M and N are manifolds, is an immersion of M in N if at each $\mathbf{p} \in M$, $D_{\mathbf{p}} f : T_{\mathbf{p}} M \to T_{f(\mathbf{p})} N$ is injective.*

Here, $D_{\mathbf{p}} f$ denotes the differential pushforward of f at $\mathbf{p}$. We also define a homotopy, similarly as in [3].

Definition 2.4. *Suppose there are two continuous functions $f, g : X \to Y$. Consider a family of maps $h_\tau : X \to Y$, $\tau \in [0, 1]$. This family of maps is a homotopy if $h_0 = f$, $h_1 = g$, and $H : X \times [0, 1] \to Y$ is continuous, where $H(x, \tau) = h_\tau(x)$. If such a homotopy exists, then f and g are called homotopic.*

We use τ instead of the conventional t here to avoid confusion when we introduce a different variable t later. Intuitively, $H(x, \tau)$ can be thought of as a continuous deformation between f and g. As τ progresses from 0 to 1, the map h_τ deforms from f to g. However, we are interested in the specific type of homotopy called regular homotopy, defined as in [2].

Definition 2.5. *A homotopy h_τ is regular if for every $\tau \in [0,1]$, h_τ is an immersion. If there exists a regular homotopy between f and g, then f and g are called regularly homotopic.*

We are now ready to define sphere eversion. From [1] we get the following definition.

Definition 2.6. *Consider the immersions $f, g : \mathbb{S}^2 \to \mathbb{R}^3$, where $f(\mathbf{p}) = \mathbf{p}$ and $g(\mathbf{p}) = -\mathbf{p}$. A sphere eversion is a regular homotopy between f and g.*

Smale proved in [6] that any two immersions of $\mathbb{S}^2$ in $\mathbb{R}^3$ are regularly homotopic, for which sphere eversion is just a special case. We will now discuss [1].

3 Eversion of a Cylinder Using Ruled Surfaces

We first begin with the cylinder parametrized by $h \in \mathbb{R}$ and $\phi \in [0, 2\pi)$. While h and ϕ do parametrize our cylinder, we do not call them parameters, which we introduce later. We will now evert this cylinder, defining cylinder eversion similar to sphere eversion in Definition 2.6. Since our final goal is not to evert the cylinder, we do not require our initial and final immersions to be perfectly circular tubes (i.e. the f and g do not have to equal $\mathbf{p}$ and $-\mathbf{p}$). We allow the two immersions to be deformed tubes, but self-intersections are still prohibited (Figure 4 below gives examples of such deformed tubes).

We start this eversion with the halfway immersion, which can be considered the halfway point duing the eversion.

$$\begin{aligned} x &= \sin\phi - h\sin\phi \\ y &= \cos\phi + h\cos\phi \\ z &= h\sin 2\phi \end{aligned} \tag{1}$$

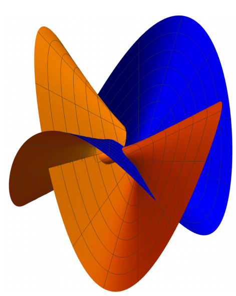

Figure 1: The halfway immersion. This was graphed using $h \in [-5, 5]$ and $\phi \in [0, 2\pi]$. The orange and blue show the two sides of the cylinder, similar to the color scheme used in [1] (our orange corresponds to the teal of [1], our blue corresponds to their orange).

Note that the immersion in Figure 1 is unbiased toward either side, making it a good halfway immersion. We now introduce the parameter t to include other stages of the eversion, where $t = 0$ corresponds to (1).

Note that t should not be strictly intepreted as time, as other parameters (which we introduce later) can vary while t remains constant, and vice versa.

$$\begin{aligned} x &= t\cos\phi + \sin\phi - h\sin\phi \\ y &= t\sin\phi + \cos\phi + h\cos\phi \\ z &= h\sin 2\phi - \frac{t}{2}\cos 2\phi \end{aligned} \tag{2}$$

At a certain value of t, keeping ϕ constant and varying h gives a ruling of the surface. We can find the distance between this ruling and the z-axis by considering the minimum value of $\sqrt{x^2+y^2}$. t and ϕ remain constant, but h will be allowed to vary.

Expanding and simplifying, we get that

$$\sqrt{x^2+y^2} = \sqrt{1+t^2+2t\sin 2\phi + 2h\cos 2\phi + h^2}$$

which is minimized when $h = -\cos 2\phi$. Substituting this value for h and simplifying yields the minimum of $\sqrt{x^2+y^2}$ to be $|t+\sin 2\phi|$.

Next we consider all the rulings and find the minimum distance between the z-axis and any of the rulings. We again minimize $\sqrt{x^2+y^2}$, now letting ϕ vary. For $|t| \leq 1$, we have ϕ satisfy $\sin 2\phi = -t$, which yields 0 to be the final minimum value. For $|t| > 1$, we have ϕ satisfy $\sin 2\phi = -\mathrm{sgn}(t)$, which yields $|t| - 1 > 0$ to be final minimum value. Thus, for $|t| \leq 1$ the immersion (which is the union of all the rulings) intersects the z-axis, but for $|t| > 1$ there is a region around the z-axis into which no ruling crosses. The case when $|t| > 1$ forms what is called the *wormhole* and brings us closer to the desired shape of a tube.

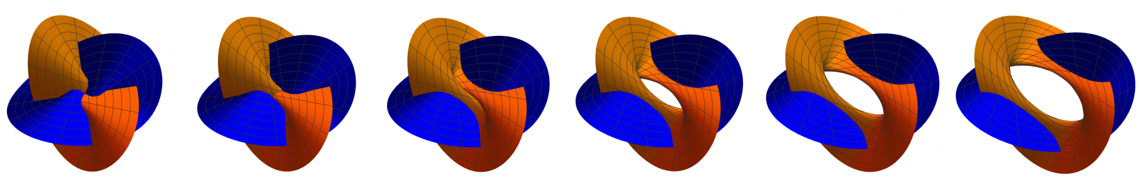

Figure 2: Several immersions described by (2), viewed from above. These six immersions are to scale relative to each other. Colors and values of ϕ, h are the same as in Figure 1. From left to right: $t = 0, \frac{1}{2}, 1, \frac{3}{2}, 2, \frac{5}{2}$.

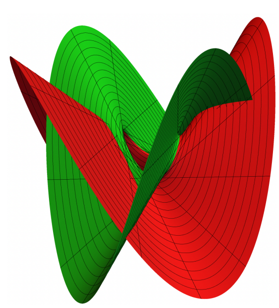

Figure 3: Another wormhole, viewed from the side at an angle. Here, $h \in [-10, 10]$ and $t = 3$. The color scheme here shows the values of h: red denotes where $h > 0$ while green denotes where $h < 0$.

In Figure 3, while the red part intersects the green part, neither the red nor green part interesects itself. As such, we want to separate the red section from the green section to remove the self-intersections. Thus, we introduce the paramter q to our expression for z, with $q \geq 0$. We get

$$z = h \sin 2\phi - \frac{t}{2} \cos 2\phi - qth$$

with $q \geq 0$. At $qt = \pm 1$, the intersections disappear (having q go from 0 to $\frac{1}{t}$ makes the intersections go to infinity). We include another parameter p, which goes from 1 to 0. $p = 0$ simplifies the parametrization, but if p is always 0 then the immersion may not be smooth at certain (t, q).

$$\begin{aligned} x &= t \cos \phi + p \sin \phi - h \sin \phi \\ y &= t \sin \phi + p \cos \phi + h \cos \phi \\ z &= h \sin 2\phi - \frac{t}{2} \cos 2\phi - qth \end{aligned} \tag{3}$$

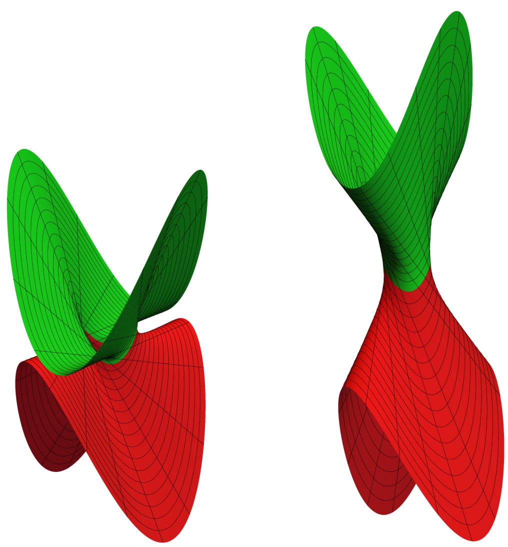

Figure 4: Like in Figure 3, $h \in [-10, 10]$ and $t = 3$. Here $p = 0$. Left, $q = \frac{1}{3}$. Right, $q = \frac{3}{4}$.

As one can see from Figure 4, increasing q stretches out the parts of the surface for large h (i.e. the parts farther from the origin) but leaves points closer in less affected. In fact, the border between the green and red regions (where $h = 0$) is not affected at all by changes in q (the reason the border looks different between Figure 3 and 4 is due to different viewing positions).

This completes the cylinder eversion; to evert the cylinder, we change t from some $t < -1$ to some $t > 1$. Along the way, we change p from 1 to 0 to 1, and change q at larger t to remove self-intersections.

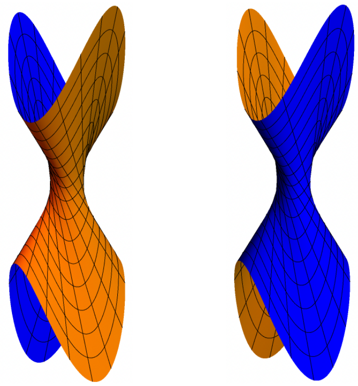

Figure 5: Both graphs use the orange-blue color scheme. The right graph depicts Figure 4. The left graph depicts Figure 4, except that $t = -3$, not $t = 3$. The left and right graphs are inversions of the other.

4 Eversion of a Sphere

Now we use the cylinder eversion to define a sphere eversion. The sphere, with radius R, is parametrized as

$$(R\cos\theta\cos\phi, R\cos\theta\sin\phi, R\sin\theta) \tag{4}$$

for $\theta \in [-\frac{\pi}{2}, \frac{\pi}{2}], \phi \in [0, 2\pi]$. In essence, finding a sphere eversion is asking the question, "At some stage during the sphere eversion, where does each point on the original sphere end up"? To answer this question, we will define a series of mappings that brings the sphere to its immersion at a certain stage, defined by the values of our parameters.

The first mapping is that of the sphere to the cylinder. For a point on the sphere defined by (θ, ϕ) as above, we map it to $\phi = \phi, h = \omega\frac{\sin\theta}{\cos^2\theta}$ for some $\omega > 0$. Changing ω does not change the shape of the cylinder. Rather, ω only affects which points on the sphere map to which points on the cylinder. For all our graphs we keep $\omega = 1$. Then we map this cylinder to the immersion given by (3). Substituting into (3) gives

$$\begin{aligned} x &= t\cos\phi + p\sin\phi - \omega\frac{\sin\theta}{\cos^2\theta}\sin\phi \\ y &= t\sin\phi + p\cos\phi + \omega\frac{\sin\theta}{\cos^2\theta}\cos\phi \\ z &= \omega\frac{\sin\theta}{\cos^2\theta}\sin 2\phi - \frac{t}{2}\cos 2\phi - qt\omega\frac{\sin\theta}{\cos^2\theta} \end{aligned} \tag{5}$$

From these two maps we currently have mapped $\mathbb{S}^2$ to a surface that is something like the figures depicted in cylinder eversion, depending on t, p, q. Now, with (x, y, z) defined as in (3), we map $(x, y, z) \to (x', y', z')$. Note that x', y', z' do not refer to any derivatives of x, y, z, but instead are defined as follows.

$$\begin{aligned} x' &= \frac{x}{(\xi + \eta(x^2 + y^2))^{1/4}} \\ y' &= \frac{y}{(\xi + \eta(x^2 + y^2))^{1/4}} \\ z' &= \frac{z}{\xi + \eta(x^2 + y^2)} \end{aligned} \tag{6}$$

Here, $\xi, \eta \geq 0$ (except when $|t| < 1$, where $\xi > 0$). The mapping $(x, y, z) \to (x', y', z')$ has the effect of taking points far from the z-axis and pushing them toward the origin. However, the push in the z-direction is larger due to the absence of the $1/4$ exponent, so the most visible effect is to push the surface toward the xy-plane.

Increasing ξ or η pushes points toward the origin as described above. However, the effect of ξ is felt more strongly for small $x^2 + y^2$, while η has a greater effect for large $x^2 + y^2$.

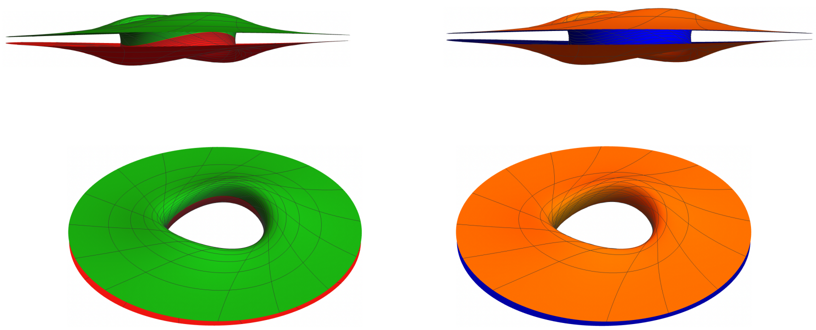

Figure 6: A graph of (6), with $t = 4$, $p = 0$, $q = 1$, $\xi = 1$, $\eta = 1$. As usual, $\phi \in [0, 2\pi]$. Finally, $\theta \in [-0.43\pi, 0.43\pi]$. Both color schemes are depicted, as well as two different viewing angles (top is from the side, bottom is from above at an angle). The hole in the middle (most obvious from the above viewpoint) corresponds to the wormhole in the cylinder eversion.

Next, we perform the final mapping. (x'', y'', z'') will correspond to our sphere eversion, as will be seen in (11).

$$
\begin{aligned}
x'' &= \frac{x'}{\alpha + \beta\left(x'^2 + y'^2\right)} e^{2z'\sqrt{\alpha\beta}} \\
y'' &= \frac{y'}{\alpha + \beta\left(x'^2 + y'^2\right)} e^{2z'\sqrt{\alpha\beta}} \\
z'' &= \frac{1}{2\sqrt{\alpha\beta}} \left(\frac{\alpha - \beta\left(x'^2 + y'^2\right)}{\alpha + \beta\left(x'^2 + y'^2\right)} e^{2z'\sqrt{\alpha\beta}} - \frac{\alpha - \beta}{\alpha + \beta} \right)
\end{aligned} \tag{7}
$$

for some $\alpha, \beta \geq 0$. For large x', y' (and thus small z'), x'' and y'' are small and z'' approaches $-\sqrt{\frac{\alpha}{\beta}}(\alpha + \beta)$. In effect, the surfaces like those in Figure 6 have their regions far from the origin wrapped around to the z-axis. For larger α and smaller β at some $|t| > 1$, the immersion appears like Figure 7, a dented sphere. For $|t| < 1$, the outer parts fold in and start to resemble Figure 8.

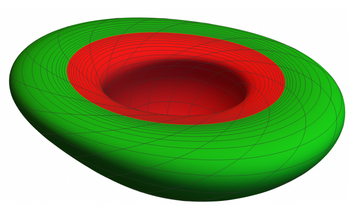

Figure 7: A graph of (7), with $t = 4$, $p = 0$, $q, \xi, \eta, \alpha = 1$, and $\beta = 0.2$. This immersion has no self-intersections, unlike the next figure. An orange-blue color scheme of this graph would appear all orange from this viewpoint.

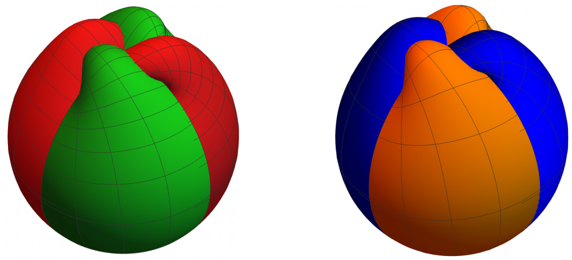

Figure 8: A graph of (7), with $t = 0$, $p = 1$, $\xi, \eta, \alpha = 1$, and $\beta = 0.04$. The value of q is irrelevant as $t = 0$. The shape of the immersion in the upper half comes from the halfway immersion of the cylinder eversion (see Figures 1, 2). In fact, this immersion could be a halfway point of the sphere eversion.

For large α and β with $t > 1$, the red region pinches in and the green region balloons out relative to Figure 7. For negative z', which is the red region when t is positive, the exponent $2z'\sqrt{\alpha\beta}$ is relatively negative, pushing x'' and y'' toward 0. Also, the $\frac{1}{2\sqrt{\alpha\beta}}$ is relatively small, pushing z'' toward 0. For positive z', $2z'\sqrt{\alpha\beta}$ is relatively large, inflating the magnitudes of x'' and y''. The prescence of $e^{2z'\sqrt{\alpha\beta}}$ in the expression for z'' means that $|z''|$ is larger in the green region.

For small α and β with $t > 1$, the surface is pushed away from the origin. The exponential $e^{2z'\sqrt{\alpha\beta}}$ is less significant. On the other hand, the denominator $\alpha + \beta(x'^2 + y'^2)$ significantly increases the magnitude of x'' and y'', as does $2\sqrt{\alpha\beta}$ for z''.

Finally, for small α and large β, see (8) and Figure 9 below.

In Figure 7, the surface takes on the form of a sphere that has been twisted and dented. This is very close to our goal of the everted sphere. We prepare our surface for its deformation into a sphere by setting $\xi = 0, \eta > 0, \alpha \to 0, \beta = 1$, which gives

$$\begin{aligned} x'' &= \frac{x'}{x'^2 + y'^2} = \frac{\eta^{1/4} x}{(x^2 + y^2)^{3/4}} \\ y'' &= \frac{y'}{x'^2 + y'^2} = \frac{\eta^{1/4} y}{(x^2 + y^2)^{3/4}} \\ z'' &= -z' = -\frac{z}{\eta\,(x^2 + y^2)} \end{aligned} \tag{8}$$

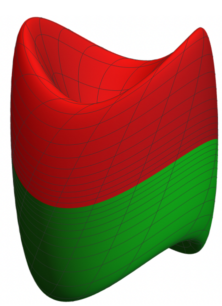

Figure 9: The graph of (8) with $\eta = 1$. An orange-blue color scheme of this graph would appear all orange from this viewing point.

Finally, we introduce the parameter $\lambda \in [0,1]$, where $\lambda = 1$ leaves the surface unchanged and $\lambda = 0$ turns the above surface into a sphere. Although we introduce λ in our definition of (x, y, z), none of the progress we have made so far is affected, as we only change λ after we have reached this point. We have

$$
\begin{aligned}
x &= \lambda \left(t\cos\phi - \omega \frac{\sin\theta}{\cos^2\theta}\sin\phi \right) + (1-\lambda)\frac{t\cos\phi}{\cos^2\theta} \\
y &= \lambda \left(t\sin\phi + \omega \frac{\sin\theta}{\cos^2\theta}\cos\phi \right) + (1-\lambda)\frac{t\sin\phi}{\cos^2\theta} \\
z &= \lambda \left(\omega \frac{\sin\theta}{\cos^2\theta}\sin 2\phi - \frac{t}{2}\cos 2\phi - qt\omega\frac{\sin\theta}{\cos^2\theta} \right) - (1-\lambda)\eta^{5/4} t|t|^{1/2}\frac{\sin\theta}{\cos^4\theta}
\end{aligned}
\tag{9}
$$

We omit the term containing p in our expressions for x and y, as $p = 0$ now. Letting λ go to 0 gives

$$
\begin{aligned}
x &= \frac{t\cos\phi}{\cos^2\theta} \\
y &= \frac{t\sin\phi}{\cos^2\theta} \\
z &= -\eta^{5/4} t|t|^{1/2}\frac{\sin\theta}{\cos^4\theta}
\end{aligned}
\tag{10}
$$

Substituting (10) into (8) gives

$$
\begin{aligned}
x'' &= \operatorname{sgn}(t)\eta^{1/4}|t|^{-1/2}\cos\theta\cos\phi \\
y'' &= \operatorname{sgn}(t)\eta^{1/4}|t|^{-1/2}\cos\theta\sin\phi \\
z'' &= \operatorname{sgn}(t)\eta^{1/4}|t|^{-1/2}\sin\theta
\end{aligned}
\tag{11}
$$

Comparing (11) to our original parametrization of the sphere (4), we see that $R = \eta^{1/4}|t|^{-1/2}$. Furthermore, positive values of t correspond to the original sphere and negative values to the inverted sphere. Thus the original sphere would appear all orange with the orange-blue color scheme, while the inverted sphere would appear all blue.

5 Summary

We have defined sphere eversion and discussed in detail a specific example of eversion, noting the effects of each parameter.

6 Further Reading

In this paper we assumed $n = 2$, but [1] covers other values of n (an integer greater than 1) that affects the rotational symmetry of the immersions. [1] also contains descriptions of self-intersections as well as the computations needed to show this eversion is smooth.

Beyond [1], there are multiple other explicit sphere eversions, including those that use Morin and Boy surfaces as halfway immersions. William Thurston has also developed a sphere eversion that uses corrugations, a method that can be generally used to make a homotopy regular. Some sphere eversions are minimax eversions, which minimize Willmore energy, a measurement of how much a surface deviates from a sphere. [7] contains a good history of sphere eversion and discusses minimax eversions in depth.

Acknowledgements

The author thanks Dr. Simon Rubinstein-Salzedo, Lucy Vuong, and Yiping Liao for their help in writing this paper.

References

[1] Adam Bednorz and Witold Bednorz. Analytic sphere eversion using ruled surfaces. *Differential Geometry and its Applications*, 64:59–79, 2019.

[2] Tobias Ekholm. Regular homotopy and total curvature I: circle immersions into surfaces. *Algebraic & Geometric Topology*, 6:459–492, March 2006.

[3] Allen Hatcher. *Algebraic Topology*. Cambridge University Press, 2001.

[4] James R. Munkres. *Topology*. Prentice Hall, 2nd edition, 2000.

[5] Ricky Reusser. Sphere eversion, June 2020. rreusser.github.io/explorations/sphere-eversion/.

[6] Stephen Smale. A classification of immersions of the two-sphere. *Transactions of the American Mathematical Society*, 90(2):281–290, February 1959.

[7] John M. Sullivan. “The Optiverse” and Other Sphere Eversions. *Visual Mathematics*, 1, 1999.